W-band Wireless Transmission based on 98 GHz Packaged Silicon Photonics Optical Clock Generator

Antonio Malacarne[1], Alberto Montanaro[1], Fawad Ahmad[2], Gaurav Pandey[2], Antonio D'Errico[3], Marco Romagnoli[1], Antonella Bogoni[2,1] and Claudio Porzi[2]

[1]*Photonic Networks & Technologies National Lab – CNIT, 56124 Pisa, Italy*

[2]*Telecommunications, Computer Engineering, and Photonics Institute (TeCIP), Scuola Superiore Sant'Anna, 56124 Pisa, Italy*

[3]*Ericsson Research, 56124 Pisa, Italy*

antonio.malacarne@cnit.it

Abstract: A fully packaged CMOS-compatible photonic integrated frequency-tunable optical clock synthesizer is used for 93 GHz wireless transmission of complex modulation formats up to 4 Gb/s data rate, with noise performance suitable for upcoming 6G networks. © 2024

1. Introduction

Emerging low-latency applications in 5G new radio and 6G networks such as digital twins, AI computing, remote surgery, etc. will require novel hardware solutions operating in the sub-THz range featuring low phase noise (PN), high signal integrity and multi gigabit per second channel capacity [1],[2]. Microwave photonics techniques offer ultra-wideband operation, wide tunability and extremely stable radio-frequency generation [3],[4]. In addition, photonics-based radiofrequency (RF) generation enables efficient distribution over low-loss and electromagnetic interference-free fiber-optics or free-space links of carrier waves in the millimeter (mm)-wave and sub-THz bands, which would otherwise suffer strong attenuation in standard coaxial cables [5]. To make the photonic approach a viable and practical alternative to standards BiCMOS solutions, system miniaturization through a suitable integration technology and optoelectronic packaging strategy is however required.

We recently reported on reconfigurable synthesis of RF oscillations up to the W-band and beyond starting from a local oscillator (LO) in the K/Ku band with PN performance in line with ideal frequency multipliers, using a photonic integrated circuit (PIC) realized in silicon-on-insulator (SOI) technology [6],[7]. Here, we use a packaged second-generation version of the silicon photonics frequency-tunable optical clock generator including an RF evaluation printed circuit board (PCB) wedge-bonded to the PIC, fiber pigtails and thermal management, in a W-band wireless transmission of complex modulated data signals up to 4Gb/s, proving the suitability of such approach for effective low-PN mm-wave band reference clock generation for B5G/6G mobile networks.

2. Frequency-Tunable Optical Clock Generation

In the photonic-integrated frequency synthesizer, part of the light injected into the PIC from an external laser source (LS) reaches an optical frequency comb (OFC) source, which is driven by a LO with frequency f_{LO} and whose spectrum spans several octaves. A single harmonic out of the comb spectrum is then isolated by a following bandpass tunable optical filter (TOF) and subsequently recombined with the original LS carrier, therefore providing at the PIC output two optical tones frequency spaced by an integer multiple of f_{LO}, i.e. Mf_{LO}, being M the selected harmonic order [6]. The circuit, realized in SOI technology through standard DUV lithography using a multi-project wafer service, exploits a 2 mm-long silicon photonics phase modulator (PM) for OFC generation, and implements a photonic-integrated TOF through a multi-cavity distributed feedback resonator (DFBR) architecture based on coupled waveguide Bragg gratings [8]. Fig 1(a) shows the PM-based OFC output spectrum with the LO off (blue) and on (red) at frequency of 20 GHz and a power level of about 1 W, together with the box-shaped transmission of the DFBR filter (dashed violet) when tuned to select the fifth-order harmonic above the carrier wavelength (M = 5). The corresponding PIC output spectrum is shown in Fig 1(b), illustrating large optical signal-to-noise ratio (OSNR) and spurious mode rejection for the two 100 GHz-spaced components. Fig 1(c) reports the PN power spectral density (PSD) measured with a signal source analyzer (SSA) in the range 1 kHz – 40 MHz of frequency offset from the carrier frequency under test, for both the reference LO signal and the generated 100 GHz RF carrier obtained by injecting the PIC output into a photodiode (PD). The offset frequency upper limit, given by the employed SSA, is in accordance with the requirements of modern wireless communication applications. On the other hand, PN contributions lower than 1 KHz, typically due to thermal and mechanical instabilities, are usually negligible in most applications, as they can be compensated by analog or digital carrier/phase recovery techniques. The plot also reports the theoretical performance at 100 GHz in case of ideal frequency multiplication by upshifting the LO trace by $10\times log_{10}(M^2)$, with M=5 for the considered multiplication factor. When comparing the measured 100 GHz PN PSD trace with the ideal multiplier, a slight deviation in the low

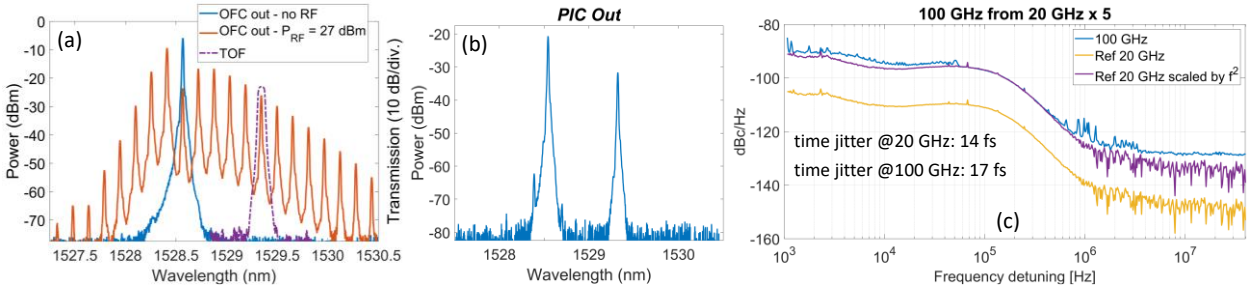

Fig. 1. PM-based OFC output spectrum with LO on and off and DFBR transmission (a), PIC output spectrum with 100 GHz-spaced optical harmonics (b) and measured phase noise power spectral densities (c).

frequency detuning range (< 50 kHz) is observed, which is attributed to the small oscillations of the DFBR filter spectral response, associated to temperature fluctuations and noise of the DC sources employed for filter tuning [7],[8].On the other hand the floor in the high frequency range is limited by the available signal-to-noise ratio (SNR), which is partially degraded by the optical amplification stage employed to rise the SSA input signal to the level required by the instrument. However, the corresponding time jitter values of 14 fs and 17 fs for the LO and 100 GHz case, respectively, confirm the limited impact on the clock performance introduced by the scheme.

3. W-band Wireless Transmission Experiment

The packaged version of the silicon photonics frequency-tunable optical clock generator can be observed in Fig. 2(a). The optoelectronic package includes an RF PCB wedge-bonded to the PIC (see Fig. 2(b)), optical access through a fiber array glued on a grating coupler array, a Peltier cell and a thermistor for thermal stabilization though an external feedback loop. The device was used for generating a low-PN 98-GHz (f_{RF}) optical clock derived from a 19.6-GHz LO. The obtained W-band optical clock has driven subsequent up conversion at 93 GHz of a complex modulated data signal generated at an intermediate frequency (IF) of 5 GHz via optoelectronic modulation and photodetection through commercial devices. The complete experimental setup to verify the performance of a W-band wireless transmission using the proposed optical clock generator for signal up-conversion, is shown in Fig. 2(c). A LS is injected into the packaged device and a polarization controller (PC) optimizes the input polarization state. After optical amplification through an Erbium-doped fiber amplifier (EDFA) and out-of-band amplified spontaneous emission (ASE) removal by an optical bandpass filter (OBPF), the optical signal subsequently passes a Mach-Zehnder modulator (MZM) driven by a data signal generated at IF by a 64 GS/s 11 GHz digital-to-analog converter. A second PC optimizes the MZM input polarization state. The MZM output is then photo-detected by a 100-GHz photodiode, and the signal term upconverted at $f_{RF} - f_{IF} = 93$ GHz that is carrying the data, is selected by a WR10 waveguide cavity filter with passband 86-94 GHz. The signal is finally amplified by a W-band amplifier and transmitted through a 2-meter wireless link using a W-band 35-dB gain antenna. An identical antenna receives the signal that is down-converted back to f_{IF} thanks to a 92-96 GHz active down-converter. Antennas exhibit this same frequency range. These limitations in term of operative frequency lead to a 2 GHz available bandwidth. A 40GS/s 12-GHz bandwidth real-time oscilloscope finally acquires the signal and subsequent offline digital signal processing (DSP) reconstructs it including error vector magnitude (EVM) measurement. The point-to-point W-band wireless transmission was tested with quadrature phase-shift keying (QPSK) modulation. The DSP tool embedded in the oscilloscope includes phase recovery and an equalization filter whose length has been optimized in the range 21-51 symbols, depending on the modulation rate. A digital raised cosine filter is also used, with bandwidth varied according to the electrical bandwidth of the received signal. The analysis includes constellation reconstruction and visualization of I or Q eye diagram, and is reported in Fig. 3(a,b) for a 0.5 Gbaud (1 Gb/s), 1 Gbaud (2 Gb/s) and 2 Gbaud (4 Gb/s) QPSK signal, with a lowest EVM measured to be 9% in the first case and for an optical power at the PD input of 0.4 dBm. In all the three cases, for

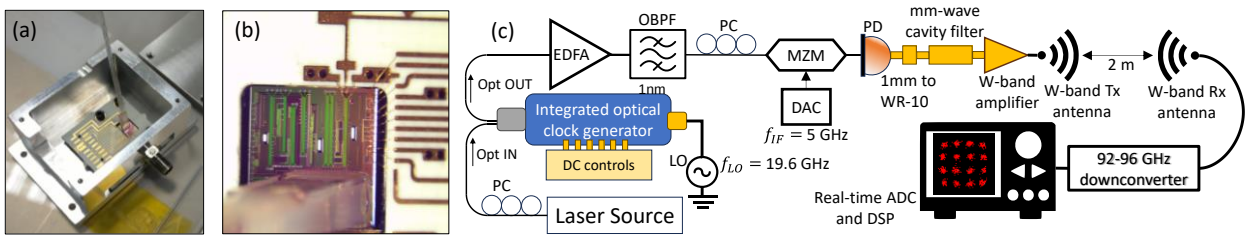

Fig. 2. Complete optoelectronic package (a), detail of PIC-to-PCB RF wedge bonds (b) and setup for the wireless transmission experiment (c).

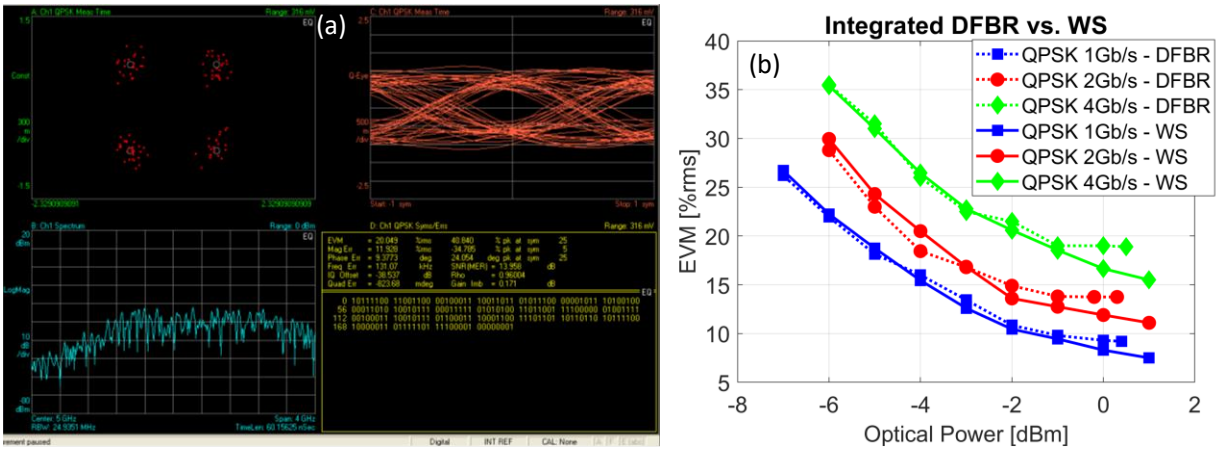

Fig. 3 Performance of 4 Gb/s QPSK transmission with reconstructed eye diagram, complex constellation, spectrum at IF and EVM statistics (a). EVM measurements versus the optical power received by the photodetector at the wireless transmitter (b).

optical power > -1 dBm, EVM performance tends to saturate, due to the available SNR level.

To benchmark the use of the integrated filter with off-the-shelf components, it was substituted with an external WaveShaper (WS) isolating two 98 GHz-spaced OFC modes. The results are also present in Fig.3(b) (continuous lines). In this case a higher optical power was available at the WS output, since the two harmonics could be independently selected, exploiting both sides of the OFC spectrum. In addition, the WS-based experiment was conducted at 1550 nm whereas the DFBR-based one is performed at around 1530 nm, the Bragg wavelength of the fabricated samples, where the EDFA noise figure (NF) is larger. Consequently, the SNR was better for the bulk WS case than the fully integrated solution. Therefore, for low optical power levels EVM performance are essentially the same, while for high powers SNR starts to be the main limiting factor, and lower EVM is measured when using the WS. However, in all cases EVM values below the hard-decision forward error correction (HD-FEC) threshold for QPSK are easily achieved [9]. To increase the output power, an improvement would consist in a two DFBR-based architecture [7]. Further efforts expected to lead to better EVM performance consist of minimizing the optical coupling losses, e.g. through edge coupling, or by employing the 1550 nm range where EDFA NF and gain are optimal.

3. Conclusion

A silicon photonics integrated circuit for flexible radiofrequency multiplication has been designed, fabricated and packaged for optical access and electrical RF/DC driving/control. The package driven by a 19.6 GHz local oscillator was used to generate a 98 GHz-spaced two-tone optical clock, employed for data signal up conversion in the W-band via electrooptical modulation and photodetection. QPSK signals with data rate up to 4Gb/s have been wireless transmitted with EVM performance confirming the effectiveness of the proposed approach in next-generation 6G wireless networks employing millimeter-wave/sub-THz carrier frequencies and multi GHz-wide data signals.

This work is partially supported by the EU under the Italian National Recovery and Resilience Plan (NRRP) of NextGenerationEU, partnership on “Telecommunications of the Future” (PE00000001 – program “RESTART”), and by the Italian Ministry of Enterprises of Made In Italy through the ISOTTICA project.

4. References

[1] P. Cerwall, et al., “Ericsson Mobility Report November 2021”, Ericsson Mobility Report 1–40, 2021
[2] “5G Evolution Toward 5G Advanced: An overview of 3GPP releases 17 and 18”, Ericsson Technology Review 14, 1–13, 2021
[3] K. Sengupta, T. Nagatsuma, D.M. Mittleman, “Terahertz integrated electronic and hybrid electronic–photonic systems”, Nature Electronics 1, 622–635, 2018
[4] T. Tetsumoto, et al., “Optically referenced 300 GHz millimitre-wave oscillator”, Nature Photonics 15 516–522, 2021
[5] P.T. Dat, et al., “Transparent Fiber–Millimeter-Wave–Fiber System in 100-GHz Band Using Optical Modulator and Photonic Down-Conversion”, Journal of Lightwave Technology, vol. 40, no. 5, pp. 1483-1493, 2022
[6] A. Malacarne, A. Bigongiari, A. D'Errico, A. Bogoni and C. Porzi, "Reconfigurable Low Phase Noise RF Carrier Generation up to W-Band in Silicon Photonics Technology," in Journal of Lightwave Technology, vol. 40, no. 20, pp. 6891-6900, 15 Oct.15, 2022.
[7] C. Porzi, et al., “Silicon Photonics Programmable Millimeter-Wave Band RF Synthesizer”, Th.B.7.6, ECOC, 2023
[8] C. Porzi, G.J. Sharp, M. Sorel, and A. Bogoni, “Silicon photonics high-order distributed feedback resonators filters”, IEEE Journal of Quantum Electronics, 56(**1**), pp.1-9
[9] Y. Fan, et al., "Fast signal quality monitoring for coherent communications enabled by CNN-based EVM estimation," J. Opt. Commun. Netw. 13, B12-B20 (2021)